2478 © 1993 The Chemical Society of Japan Bull. Chem. Soc. Jpn., 66, 2478—2491 (1993) [Vol. 66, No. 9

Molecular Dynamics Simulation of Aqueous MNO_3 (M=Li, Na, K, Rb, and Cs) Solutions

Yosuke KATAOKA†
Department of Chemistry, Faculty of Science, Kyoto University, Oiwake-cho, Kitashirakawa, Sakyo-ku, Kyoto 606-01
(Received March 8, 1993)

To understand the anisotropy, cation dependence, and concentration dependence of the orientational relaxation time of the nitrate ion, the structure and molecular motion were studied by molecular dynamics simulation of MNO_3 (M=Li, Na, K, Rb, and Cs) solutions. The interaction parameters determined for the molten salt were used between the ions. The Carravetta–Clementi potential was assumed for the water–water pair. An empirical combination rule was adopted in the water-ion interactions. Simulations were done at several volumes corresponding to the normal density and low pressures. The temperature was 300 K and the concentrations was 1 or 2 $\mathrm{mol\,kg^{-1}}$. The distribution of water molecule is almost isotropic around the nitrate ion. No water molecules are found which move in strong correlation with the rotation of the nitrate ion. The calculated orientational relaxation time of the nitrate ion is in agreement with the experimental results qualitatively with respect to its anisotropy, cation dependence, and concentration dependence. These were analyzed by the potential energy of the species around the nitrate ion. The anisotropy of the relaxation time was due to the anisotropic charge distribution in the nitrate ion, as demonstrated by several models.

The orientational relaxation of the nitrate ion was studied experimentally (NMR,[1—4] Raman,[5—9]) and light scattering[10]) in dilute aqueous MNO_3 (M=Li, Na, K, Rb, and Cs) solutions. These studies have revealed the following points of interest:

(1) The anisotropy[1—4] of the relaxation time of the planar nitrate ion is different from the ordinary case, for instance benzene[11]) in a solution.

(2) The relaxation time generally decreases in the order of Li, Na, K, Rb, and Cs.[3,4])

(3) The relaxation time increases linearly with increasing concentration.[3,4]) The relative increase amounts to as much as 0.3 by addition of the salt to a level of only 0.02 in mole fraction.

As for concentrated solutions, X-ray[12]) and neutron[13]) scattering experiments were reported. The anisotropy of the relaxation was not explained by the continuum theory,[3]) which predicts a linear concentration dependence.[14]) This theory gives a different size dependence on the counter cation from that in the experimental slope of the relaxation time as a function of concentration (Fig. 1 in Ref. 14). The hydration energy was obtained by high pressure mass spectroscopy,[15]) and was compared with an empirical quantum chemical calculation.[15])

We are interested in obtaining microscopic information on this solution to understand the above three points by molecular dynamics simulations. The system comprises 512 molecules or ions, and the concentration is 1 or 2 $\mathrm{mol\,kg^{-1}}$. The ion–ion pair interaction determined for the molten salt[16,17]) is used. The interaction between the solvent water molecules is the Carravetta–Clementi potential[18]) which can reproduce

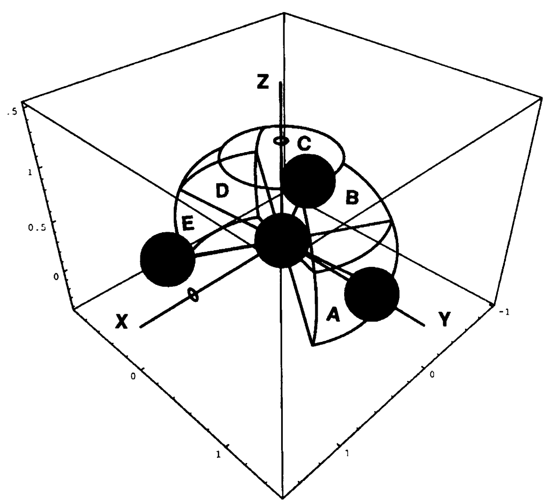

Fig. 1. Standard orientation of nitrate ion.

the thermodynamic[19]) and transport[20]) properties of liquid water. In the water-ion interactions, an empirical combination rule is assumed.

The anisotropy and the cation dependence of the relaxation time will be examined to see that its trend and its order of magnitude are in agreement with the experiments. The radial distribution functions, coordination number, and the angular distribution of water molecules around the nitrate ion will be studied as the basis for the following discussions. The correlation of motion between the nitrate ion and water will be calculated. The molecular distance of water from the nitrate ion will be also monitored.

On the basis of the above calculations, the main factor will be searched which determines the orientational relaxation time of the nitrate ion on a microscopic level.

Model Potential

For simplicity, a two-body interaction is assumed.

†Present address: Department of Materials Chemistry, College of Engineering, Hosei University, 3-7-2 Kajinocho, Koganei, Tokyo 184.

The ion–ion potential is expressed with the atomic distance r as follows;[16,17a)]

$$u_{ij}(r)=\frac{z_i z_j e^2}{r}+A_{ij}\exp\left(-B_{ij}r\right). \quad (1)$$

We use the interaction parameters given for the molten $LiNO_3$ and $RbNO_3$ salts.[16,17a)] (The charge distribution in the nitrate ion is shown as model 2 in Table 3, which is given by an ab initio molecular orbital calculation.[17b)]) The potential function of the Carravetta–Clementi model[18)] for water–water pair has the same form as Eq. 1. Only the O–H pair is written as below;

$$\begin{aligned}u_{ij}(r) = &\frac{z_i z_j e^2}{r}+A^1{}_{ij}\exp\left(-B^1{}_{ij}r\right)\\ &+A^2{}_{ij}\exp\left(-B^2{}_{ij}r\right), \quad \text{(O–H)}. \end{aligned} \quad (2)$$

An empirical combination rule is assumed between a water molecule and an ion. In order to use a combination rule, we define a size parameter σ_{ii} by the next equation;

$$\frac{A_{ii}}{A_0}\exp\left(-B_{ii}\sigma_{ii}\right)=1, \quad (3)$$
$$A_0=0.5\times10^{-19}\,\mathrm{J}.$$

Here the value of A_0 is the order of magnitude of an ion–ion interaction energy. The numerical values of σ_{ii} are given in Table 1. This parameter has a meaning of the effective diameter of an atom or ion. The size parameter σ_{ii} of a cation in Table 1 is the Tosi and Fumi parameter[16)] expressed in the form in Eq. 1.

The employed combination rule for an i–j pair is:

$$A_{ij}=\left(A_{ii}A_{jj}\right)^{1/2}, \quad (4)$$

$$B_{ij}=\frac{\log\left(\frac{A_{ij}}{A_0}\right)}{\frac{(\sigma_{ii}+\sigma_{jj})}{2}}. \quad (5)$$

The combination rule for the energy parameter A_{ij} given by Eq. 4 is frequently used. The parameter B_{ij} includes the size and energy parameters. For this reason the size parameter σ_{ij} is first obtained as $(\sigma_{ii}+\sigma_{jj})/2$, then the relation of σ_{ii} and B_{ii} is assumed as Eq. 5. This combination rule is used for (H, O–M^+) and (O/H_2O–N, O/NO_3^-) pairs. In the (H/H_2O–O/NO_3^-) pair, Eq. 2 is used tentatively, which is valid for a hydrogen bond in water.

The standard orientation of the nitrate ion is illustrated in Fig. 1. The pair interaction energies for the representative configurations are shown in Fig. 2, where the relative orientations are given in Fig. 3. These orientations are chosen because the energy minimum is found in each pair. The water–water pair has the symmetrical eclipsed configuration as shown in Fig. 3 in Ref. 19.

Table 1. Parameters A_{ii} and σ_{ii} in the Interaction between Atoms i

i=Atom/Species	$A_{ii}/10^{-19}$ J	σ_{ii}/Å
N/NO_3^-	30.656	1.400
O/NO_3^-	354.33	2.100
H/H_2O	248.61	1.615
O/H_2O	31555.91	2.324
Li^+	158.51	1.632
Na^+	507.06	2.340
K^+	2432.00	2.926
Rb^+	6740.98	3.174
Cs^+	83840.73	3.440

1 Å=10^{-10} m.

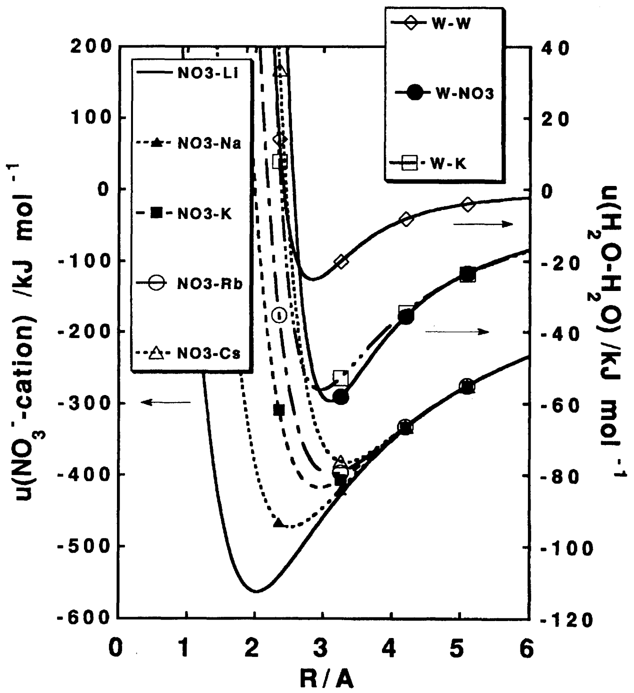

Fig. 2. Pair potential energy as a function of the molecular distance R. 1 Å=0.1 nm. The relative orientations are fixed as in Fig. 3. The interaction energies between nitrate ion and a cation are given by the left-hand y-axis, and those for other pairs by the right-hand y-axis.

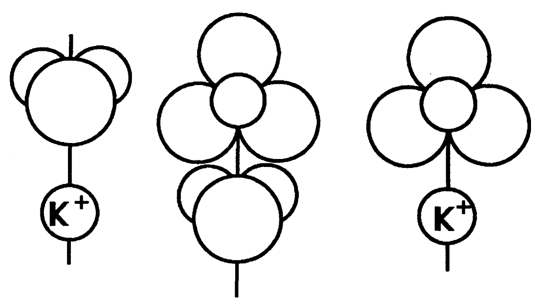

Fig. 3. Relative orientations for the pair energy plots in Fig. 2. The pair energy is minimum at the configuration shown here.

As the energy between the nitrate ion and a cation is much larger than these for other pairs in magnitude, it is shown by the left-hand y-axis.

The nitrate ion–water interaction is probably the most important to understand the orientational relaxation of the nitrate ion. This is examined in more detail below. In Fig. 4, a water molecule is put on the same xy plane as the nitrate ion. The origin of the axis is the position of the N atom. The orientation of the water is optimized to minimize the pair energy. The contour map of the minimized energy is shown in Fig. 4. The energy of the innermost curve is zero. The energy changes by 6 kJ mol^{-1} when the water goes outward to the next line. The energy minimum points are found at $(x, y, z)=(0, -0.3\text{ nm}, 0)$ and there are three equivalent points because of the 3-fold symmetry of the nitrate ion. The minimum energy is -60 kJ mol^{-1}. The valley of the minimum energy has a full-width angle of 40° as viewed from the origin.

Figure 5 is plotted for comparison. A water molecule sits on the yz plane and the nitrate ion is on the xy plane as before. The valley of the minimum energy has a full-width angle of 128° in this case, and is much wider than that in Fig. 4.

The enthalpy change of the nitrate ion by hydration is 71 kJ mol^{-1} as determined by high pressure mass spectroscopy.[15] The empirical molecular orbital calculation gives an energy of 99 kJ mol^{-1}.[15] The minimum energy -60 kJ mol^{-1} in our model is comparable with those values, although the minimum energy configuration is different from that by a quantum chemical result.[15]

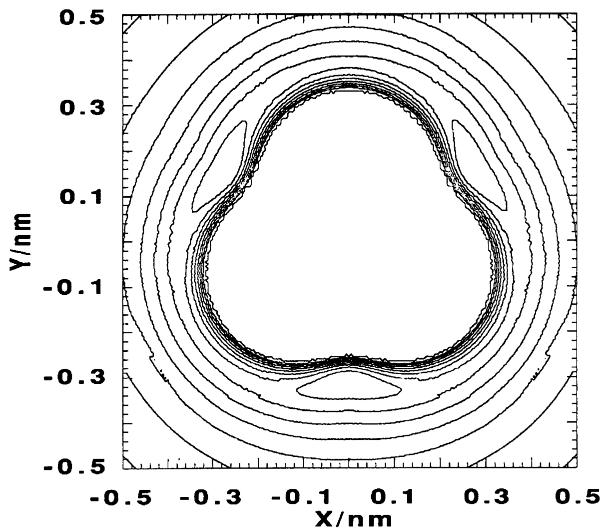

Fig. 4. Contour map for the nitrate ion–water pair energy. The nitrate ion is on the xy plane with the nitrogen atom at the origin. The orientation of nitrate ion is fixed. At each position of a water molecule on the xy plane, its orientation is optimized to minimize the pair energy. The energy minimum point is $(x, y, z)=(0, -0.3\text{ nm}, 0)$. The energy of the innermost curve is zero.

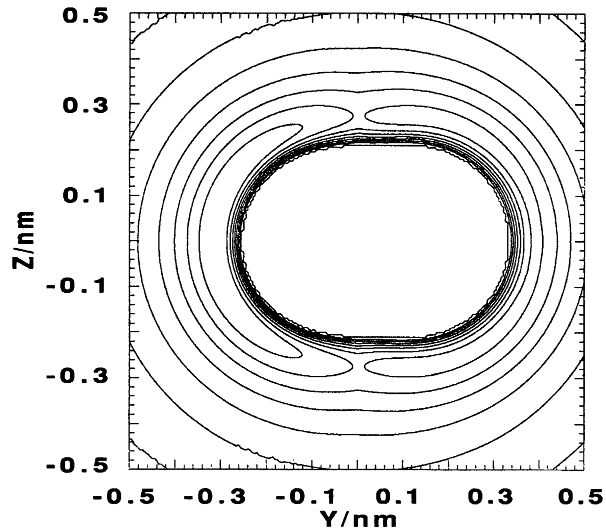

Fig. 5. Contour map for the nitrate ion–water pair energy. Nitrate ion is on the xy plane (see Fig. 4), and water is on the yz plane.

Molecular Dynamics Simulation

The water molecule is rigid in the present model.[18] The molecular dynamics (MD) method is essentially the same as the previous one.[19,20] The program MDMPOL coded by Smith and Fincham[21] is used as the basis of the present program. The electrostatic forces and energy were calculated by the Ewald method. The short range terms were cut off at half of the MD cell width. The CPU time was 0.29 s per step on a FACOM VP-400E vector processor at the Kyoto University Data Processing Center.

The time step used in this work was 0.5 fs. In the first 5 ps run, the temperature was assumed to be to 300 K. The 10 ps MD runs were repeated several times to obtain statistical averages. The simulated states are summarized in Table 2, with the solute, time range of simulation t, volume V, concentration c, temperature T, pressure P, and the potential energy E. The numbers of the species A in the MD cell N(A) are as follows:

$$N(\text{nitrate ion}) = 9,\ N(\text{cation}) = 9,\ N(\text{water}) = 494,\ \text{or}$$
$$N(\text{nitrate ion}) = 18,\ N(\text{cation}) = 18,\ N(\text{water}) = 476. \tag{6}$$

The upper and lower cases are called as 1 and 2 mol kg^{-1} solution, respectively.

Orientational Relaxation Time

In this section we examine whether the calculated relaxation time of the nitrate ion is in agreement with the experiments. The anisotropy, cation dependence, and the order of magnitude are the questions.

The relaxation time was obtained by time integration

Table 2. Parameters Adopted for MD Simulation

Solute	$c/\mathrm{mol\,kg^{-1}}$	t/ps	$V/\mathrm{cm^3\,mol^{-1}}$	T/K	P/MPa	$E/\mathrm{kJ\,mol^{-1}}$
$LiNO_3$	1	100	18	309	226	−50.57
$LiNO_3$	1	10	19	299	101	−50.70
$LiNO_3$	1	40	20	304	30	−50.19
$LiNO_3$	2	20	19	302	70	−62.73
$LiNO_3$	2	60	20	300	17	−62.65
$NaNO_3$	1	100	18	304	260	−48.74
KNO_3	1	110	18	300	305	−47.72
KNO_3	1	50	19	306	179	−47.25
KNO_3	1	40	20	301	81	−47.36
KNO_3	1	40	21	300	5	−47.17
KNO_3	2	30	18	304	394	−56.69
KNO_3	2	30	19	300	217	−56.59
KNO_3	2	30	20	307	119	−56.02
KNO_3	2	80	21	300	27	−56.18
$RbNO_3$	1	80	18	299	329	−47.54
$CsNO_3$	1	90	18	309	366	−46.88
$CsNO_3$	2	20	22	303	15	−54.83
H_2O	0	70	18	298	248	−38.93
H_2O	0	70	20	304	43	−38.01

Table 3. Anisotropy of the Relaxation Time τ for Several Models

Model	Charge/e N	Charge/e O	$\tau_x=\tau_y/\mathrm{ps}$	τ_z/ps	τ_x/τ_z	Error bar in τ_x/τ_z
1	0	−0.33	0.809	0.535	1.51	0.19
2	0.66	−0.55	0.681	0.650	1.05	0.05
3	−1	0	4.84	6.66	0.73	0.04
4	0	0	0.437	0.428	1.02	0.05
5	0.66	−0.55	0.657	0.615	1.07	0.06

The moment of inertia of NO_3^- is as follows; $I_x = I_y = 6.22\times10^{-46}$ kg m^2, $I_z = 12.5\times10^{-46}$ kg m^2 (Model 1—4), $I_x=I_y=I_z=8.30\times10^{-46}$ kg m^2 (Model 5).

of the relaxation function $\Psi_\alpha(t)$:

$$\Psi_\alpha(t) = \langle P_2(\cos\theta_\alpha(t))\rangle, \quad (\alpha = x,\ y,\ z) \tag{7}$$

where $\theta_\alpha(t)$ is the angle between the direction of the molecular α-axis at time t and 0. The function P_2 is the second order Legendre polynomial. This type of relaxation function was used to obtain the relaxation time derived from NMR and Raman scattering experiments.[3,6]

Some examples of the relaxation functions are shown in Fig. 6. Because of the 3-fold symmetry, the functions $\Psi_x(t)$ and $\Psi_y(t)$ should be equal. The functions $\Psi_z(t)$ and $(\Psi_x(t)+\Psi_y(t))/2$ are described. The calculated function is in qualitative agreement with the Raman result.[6] A more detailed comparison will be done in the section of the coordination number.

The relaxation time is given by:

$$\tau_\alpha = \int_0^\infty \Psi_\alpha(t)\mathrm{d}t. \tag{8}$$

The relaxation time is plotted as a cation dependence

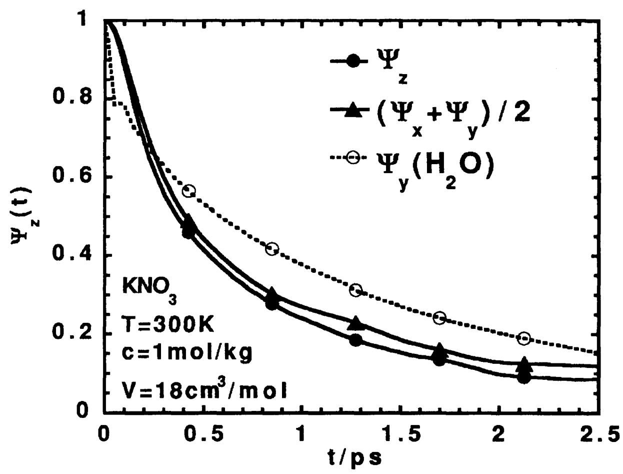

Fig. 6. Plot of the orientational relaxation function versus time t for KNO_3 solution. T=300 K, c=1 mol kg^{-1}, V=18 cm^3 mol^{-1}.

in Fig. 7 for a molar volume V=18 cm^3 mol^{-1}, temperature T=300 K, and concentration c=1 mol kg^{-1}. The relaxation time τ_{xy} means $\tau_x=\tau_y$ in this figure. The experimental result is also shown for comparison. (The relaxation time τ_z is called $\tau_\perp$ in Ref. 3.) The order of magnitude of the relaxation time is in agreement with experiment.[3] The cation dependence is reproduced on the whole. The obtained anisotropy has the same inequality $\tau_{xy}>\tau_z$ as the experiment[3] although the ratio τ_{xy}/τ_z is close to unity. This ratio depends strongly on the charge distribution in the nitrate ion as seen in Table 3.

The solvent water has a larger self-diffusion coefficient than by the macroscopic observation.[19] The

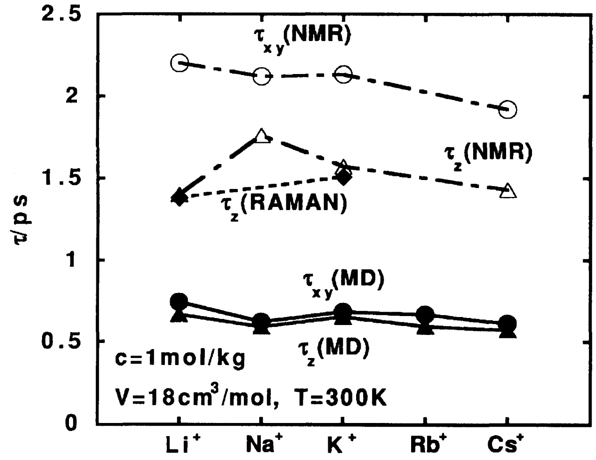

Fig. 7. Orientational relaxation time of nitrate ion. $T=300$ K, $c=1$ mol kg^{-1}, $V=18$ cm^3 mol^{-1}. The data of τ(NMR) and τ(RAMAN) are from Ref. 3.

Carravetta–Clementi water has a smaller shear viscosity than the experimental value.[19] These properties are responsible for the short relaxation time in the present solution.

The orientational relaxation time of water is a measure of the lifetime of the hydrogen bonded water structure. The orientational relaxation function of the y-axis of water molecule is also shown in Fig. 6. The value is an average by the all water molecules in the solution. (The standard orientation of the water molecule is to be shown in Fig. 11.) From this figure it is seen that the relaxation time of water in this solution is longer than that of the nitrate ion. It will be shown that the relaxation time of water in the MNO_3 solution is slightly longer than that in pure liquid in Fig. 19. This trend is consistent with an observation that the orientational relaxation time in pure water, 2.0—2.7 ps by NMR,[22—24] is longer than the relaxation time of the nitrate ion.

Structure and Energy Analysis of Solution

In the foregoing section it was shown that the present model reproduces the relaxation time qualitatively. Below we examine the thermodynamic properties, structure, and energy distribution in the solution.

Thermodynamic Properties. Table 2 gives how the average potential energy E and pressure P depend on the nature of cation at molar volume $V=18$ cm^3 mol^{-1}, temperature $T=300$ K, and concentration $c=1$ mol kg^{-1}. The energy and pressure increase in the order:

$$Li^+ < Na^+ < K^+ < Rb^+ < Cs^+. \tag{9}$$

The energy is lower than that of pure water due to an electrostatic interaction. The pressures of the solution distribute around the value of pure liquid (Table 2).

Structure Analysis. The radial distribution functions and running coordination number are illustrated in Figs. 8 and 9, respectively. The counter cation dependence of the coordination number is shown in Fig. 10. The coordination number in the first shell is calculated for the first minimum of the radial distribution function. The hydration number of the nitrate ion is 10—11, and that of a cation is 5—11 in fair agreement with the MD result[25—27] on aqueous alkali halide solutions.

The radial distribution function of the nitrate ion–cation pair is very large around the first peak. However, the coordination number of the cation around the nitrate ion is about 0.5 because of the low concentration (1 mol kg^{-1}). This number of ion contact is in agreement with the value 0.12—0.3 estimated by Yokoyama[28] on the basis of the ion-association constant.[29] Kato et al.[6] analyzed the short time part of the relaxation function ($t<0.2$ ps) and obtained an effective moment of inertial of the nitrate ion in a KNO_3 solution. This value is explained by the coordination number 0.24. From these we believe that the calculated coordination number of the cation around the nitrate ion is not far from the real.

We must be careful in comparing the atomic radial distribution function (Fig. 8b) with X-ray[12] and neutron[13a,13b] scattering experiments directly, because these are observed for concentrated samples (5—8.6 mol kg^{-1}). Neilson and Enderby observed peaks at 0.205 and 0.265 nm in N/NO_3^-–D/D_2O pair by neutron scattering on a 7.8 mol dm^{-3} aqueous $NaNO_3$ solution.[13a] Yamaguchi et al. reported a peak at 0.28 nm in N/NO_3^-–D/D_2O pair by neutron scattering on a 8.6 mol dm^{-3} aqueous $LiNO_3$ solution.[13b] A peak at 0.27 nm is observed by the present MD simulation on a 2 mol kg^{-1} aqueous KNO_3 solution (Fig. 8b). This is assigned to the second peak by Neilson and Enderby. The peak at around 0.205 nm is tentatively assigned to that in the O/NO_3^-–H/H_2O pair in the present study (Fig. 8b). In the N/NO_3^-–O/D_2O pair Neilson and Enderby found peaks at 0.265 nm and 0.340 nm.[13a] There is a peak at 0.38 nm in Yamaguchi et al.'s observation on the same atomic pair.[13b] The peak at 0.36 nm corresponds to the second peak at 0.340 nm.[13a] The nearest neighbor pair at 0.265 nm observed by neutron scattering[13a] is not found in the N/NO_3^-–O/D_2O pair but is close to a peak in the O/NO_3^-–H/H_2O pair (Fig. 8b).

Three peaks (0.225, 0.285—0.290, and 0.340 nm) are reported for two concentrated (5 and 7 mol dm^{-3}) aqueous solutions of $NaNO_3$ by X-ray diffraction.[12] Caminiti et al. assigned the 0.285—0.290 nm peak to O/NO_3^-–O/H_2O and O/H_2O–O/H_2O.[12] The first peaks in these pairs are both 0.29 nm in Fig. 8. (The center of mass almost coincides with the position of the oxygen atom in the water molecule.) The peak at 0.340 nm corresponds to the peak at 0.36 nm in the N/NO_3^-–O/H_2O pair distribution function (Fig. 8b). A peak at around 0.225 nm is not found in the pairs between O and N in the present calculation. This peak includes

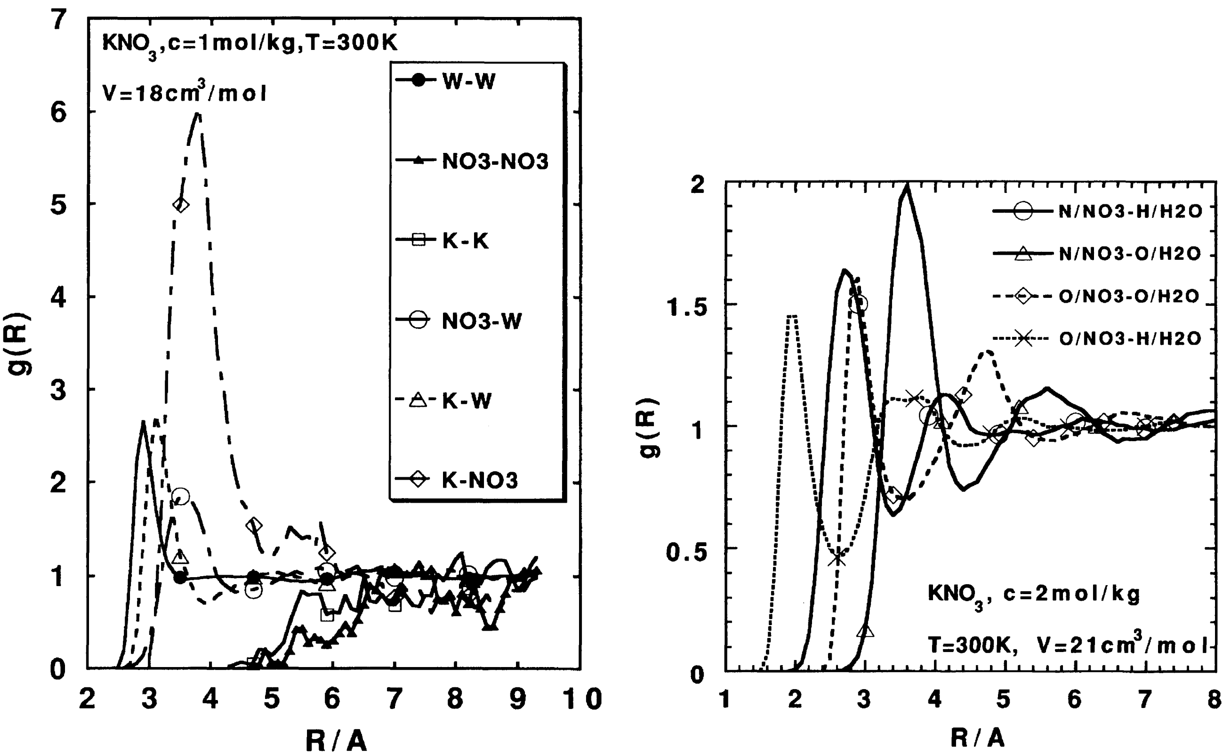

Fig. 8. Molecular radial distribution function $g(R)$ for KNO_3 solution. a) 1 Å=0.1 nm. T=300 K, c=1 mol kg^{-1}, V=18 cm^3 mol^{-1}. The symbol W denotes water. b) 1 Å=0.1 nm. T=300 K, c=2 mol kg^{-1}, V=21 cm^3 mol^{-1}.

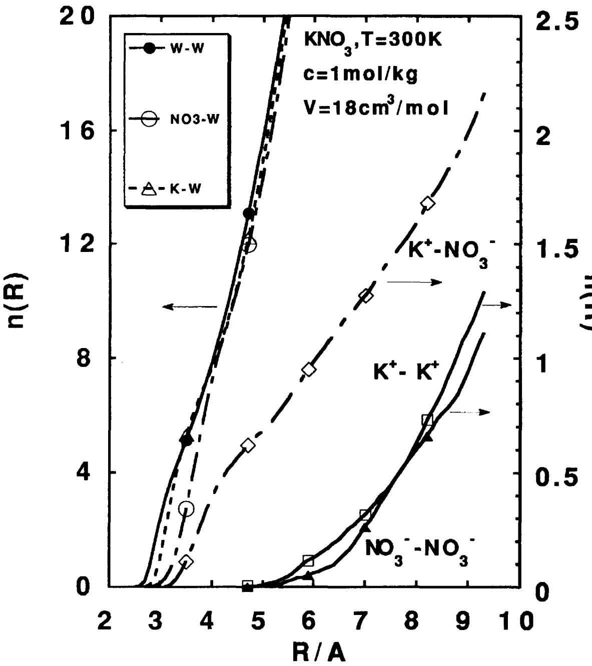

Fig. 9. Running coordination number $n(R)$ for KNO_3 solution. 1 Å=0.1 nm. T=300 K, c=1 mol kg^{-1}, V=18 cm^3 mol^{-1}. The symbol W means water.

the O–O distance within the nitrate ion.[12]

The angular distributions of the species A in the first neighbor shell of the other species B, $f(\theta)$, $f(\phi)$(A/B) are plotted in Fig. 11. The polar coordinate of the position vector of a water molecule seen from the molecular axis of the nitrate ion is expressed as (r, θ, ϕ). The distribution of θ or ϕ is plotted as $f(\theta)(H_2O/NO_3^-)$ or $f(\phi)(H_2O/NO_3^-)$. The other functions are defined in a similar way. The distribution of the nitrate ion around the water molecule has a maximum at around θ=90 degrees and ϕ=56 degree. The distribution of the cation around the nitrate ion has a maximum at around θ=90 degrees and ϕ=60 degree. On the contrary, the distribution of water is almost uniform around the nitrate ion. The hydration structure of the nitrate ion discussed by Nicholas and Wasylishen[2] does not apply to the solution considered here.

Energy Distribution. The pair-energy distribution is shown in Fig. 12. There are two peaks in the distribution functions in Fig. 12; the one corresponds to the stable pair and the other is the broad one around O. Only 3.4% of the overall nitrate ion–water pairs has an energy lower than −25 kJ mol^{-1}.

The binding energy (BE) of the i-th molecule is defined by the summation of the pair-potential u_{ij} as follows:

$$BE(i) = \sum_j u_{ij}. \tag{10}$$

The distributions of the $BE(i)$ are plotted in Fig. 13. The binding energy means the potential energy of each molecule. The binding energy of the nitrate ion has a large absolute value compared with that of water. The cation dependence of BE is depicted in Fig. 14. In this figure, $10BE$(water) is plotted instead of BE(water) for

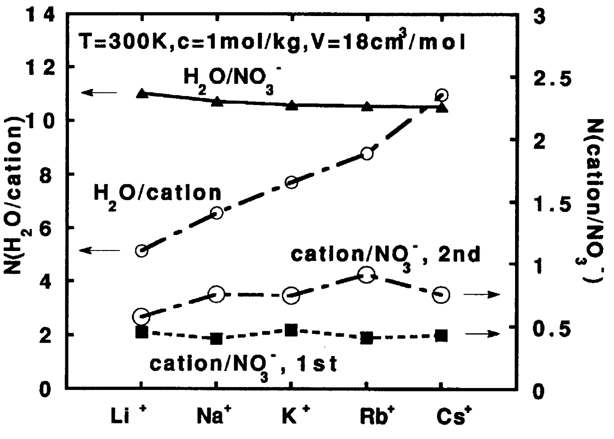

Fig. 10. Coordination number N(A/B), denoting the number of species A around B. $T=300$ K, $c=1$ $\text{mol}\,\text{kg}^{-1}$, $V=18$ $\text{cm}^3\,\text{mol}^{-1}$.

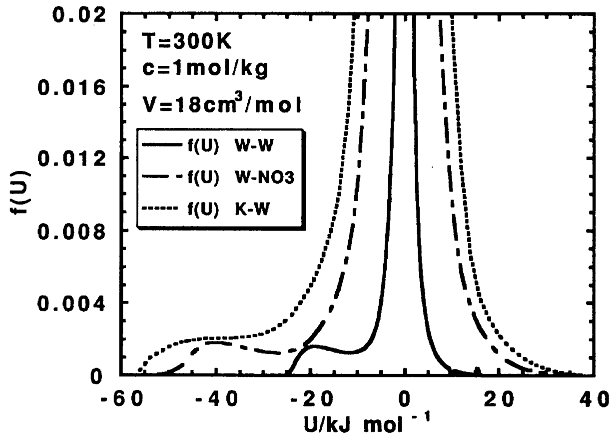

Fig. 12. Pair energy distribution for KNO_3 solution. $T=300$ K, $c=1$ $\text{mol}\,\text{kg}^{-1}$, $V=18$ $\text{cm}^3\,\text{mol}^{-1}$. The symbol W denotes water.

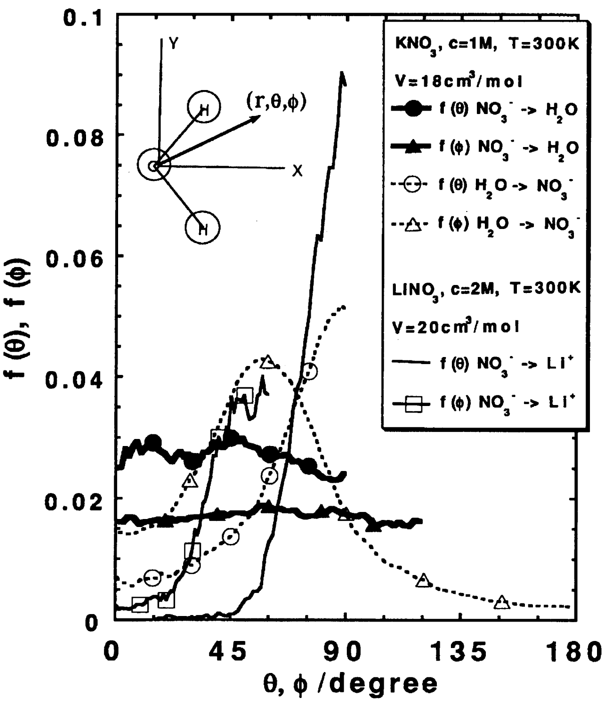

Fig. 11. Distribution of the position vector B→A of species A seen from B (see text).

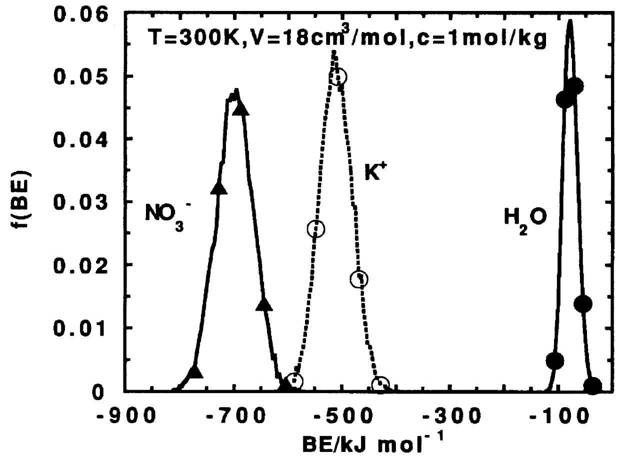

Fig. 13. Binding energy (BE) distribution for KNO_3 solution. $T=300$ K, $c=1$ $\text{mol}\,\text{kg}^{-1}$, $V=18$ $\text{cm}^3\,\text{mol}^{-1}$.

convenience. The strong cation dependence is found in BE(cation) as readily expected from the size of the cation. In contrast, the cation dependence of BE(nitrate ion) and BE(water) is weak.

A more detailed analysis is shown in Fig. 15, where the BE of the water in the first neighbor shell of ion is plotted. These are compared with that in pure liquid. The average BE(water) in the solution is almost the same with that in pure liquid. The BE(water/NO_3^-) other than the $LiNO_3$ solution is higher than BE(water) in pure liquid.

The average pair energy of the water-ion pair is given in Fig. 16, where the water is in the first neighbor shell of ion. It is interesting that the average pair energy of the water–nitrate ion pair depends weakly on the nature of cation (Fig. 16).

Rotation of Nitrate Ion

The rotational motion of the nitrate ion will be examined in the section. The correlation between the rotation of the nitrate ion and the motion of the water in the first neighbor will be sought.

The normalized time correlation function of the angular velocity of the nitrate ion is depicted in Fig. 17. The decay of the z component ($t<0.4$ ps) is slower than other components. This feature is consistent with the anisotropic orientational relaxation function in Fig. 6.

Now we examine whether any water molecules move cooperatively with the rotation of the nitrate ion. The result is shown in Fig. 18. The motion of the first neighbor water molecules in the orientation A and E (Fig. 1) around the nitrate ion are given, because these are stable orientations as seen in Figs. 1, 4, 5, and 22. We attempt to see how the water in the E direction at time

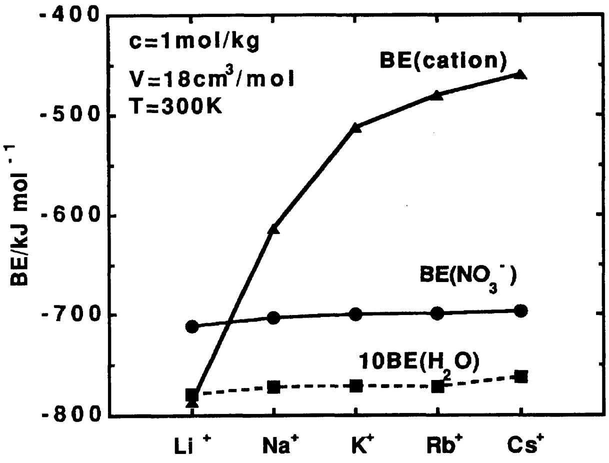

Fig. 14. Cation dependence of the binding energy of species A, BE(A). 10BE(water) is shown instead of BE(water). T=300 K, c=1 mol kg^{-1}, V=18 cm^3 mol^{-1}.

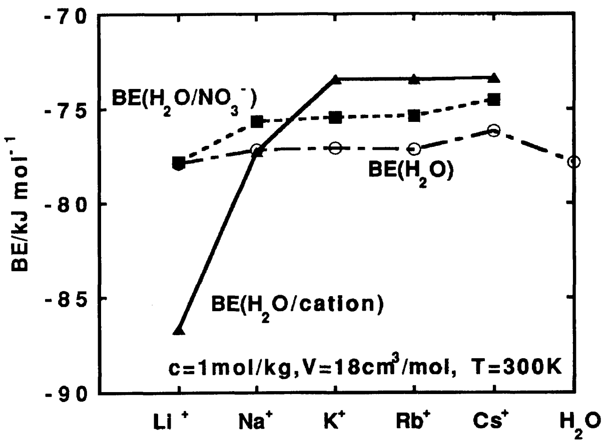

Fig. 15. Binding energy of water in the vicinity of ion A, BE(water/A). T=300 K, c=1 mol kg^{-1}, V=18 cm^3 mol^{-1}.

0 moves when the ion rotates in the xy plane of the ion (Figs. 1 and 4). If the water molecule also moves in the same plane, the direction vector of the water that is seen from the nitrate ion will show a strong correlation with the rotation of the nitrate ion. The projection to the xy plane of the direction vector was examined in the actual calculations. The angle between the projected vector at t=0 and t is $\theta(t)$. The average $<\sin\theta(t)>$ is shown in Fig. 18 by the solid curve. It is found that this quantity does not increase so much compared with the rotated angle of x-axis of the nitrate ion that the monitored water coordinated.

Another case is plotted by dotted lines in Fig. 18. In this case, the direction vector of water was projected to the yz molecular plane of the nitrate ion. The motion of the vector is compared with the rotated angle of y-axis. No strong correlation is found as seen in Fig. 18. The water molecules coordinated in the other direction were also examined. The results were similar to Fig. 18.

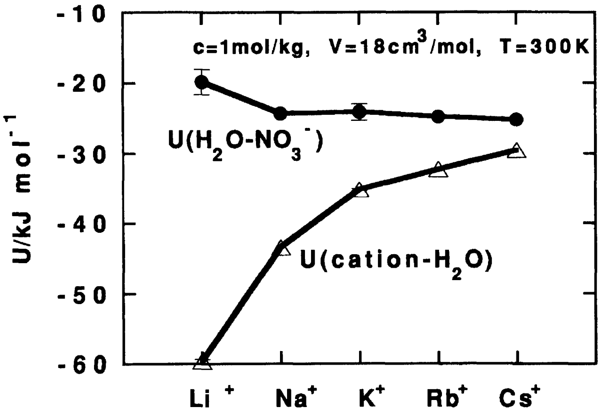

Fig. 16. Average pair energy between water and ion A, U(water-A). The water is the neighbor of ion. T=300 K, c=1 mol kg^{-1}, V=18 cm^3 mol^{-1}.

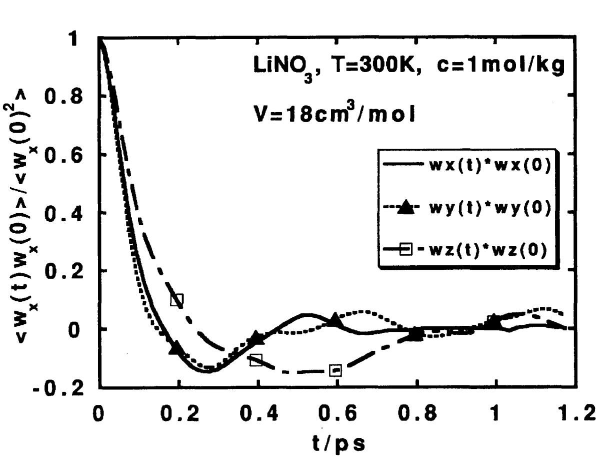

Fig. 17. Normalized time correlation function of the angular velocity of nitrate ion for $LiNO_3$ solution. T=300 K, c=1 mol kg^{-1}, V=18 cm^3 mol^{-1}.

This observation is consistent with the discussion by Perrot et al.[7] that "end-over-end rotation (of the threefold symmetry-axis) of the nitrate anions does not carry along tightly bound water molecules."

The rotational relaxation time τ_z of water and τ(nitrate ion)=$(\tau_x+\tau_y+\tau_z)/3$ are plotted against the cation in Fig. 19. The relaxation time of the water in the solution is longer than that in pure water. The relaxation time of water is longer than that of the nitrate ion.

Self-Diffusion Coefficient

The translational motion in the solution is analyzed here in terms of the self-diffusion coefficient. The cation dependence of the self-diffusion coefficient D is shown in Fig. 19. This dependence is weak and its value is close to that of pure liquid. The self-diffusion coefficient of water is larger than that of ions. This feature is in agreement with experiments.[30—32] The relations:

$$\tau(\text{water}) > \tau(\text{nitrate ion}), \tag{11}$$

$$D(\text{water}) > D(\text{nitrate ion}), \tag{12}$$

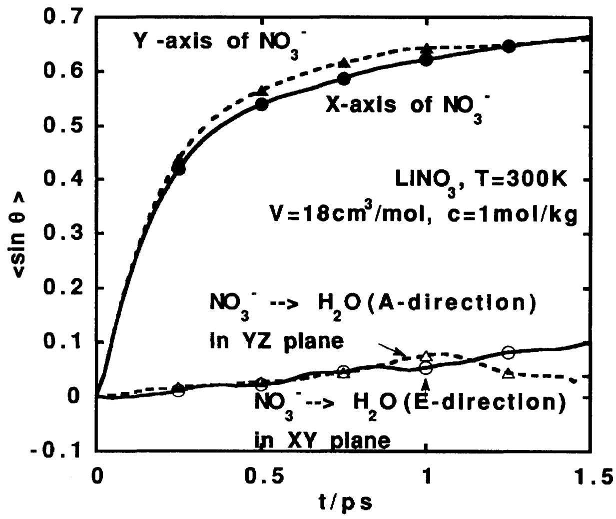

Fig. 18. Correlation between the rotation of the nitrate ion axis and the position vector of water seen from nitrate ion (see text) for $LiNO_3$ solution. $T=300$ K, $c=1$ mol kg^{-1}, $V=18$ cm^3 mol^{-1}.

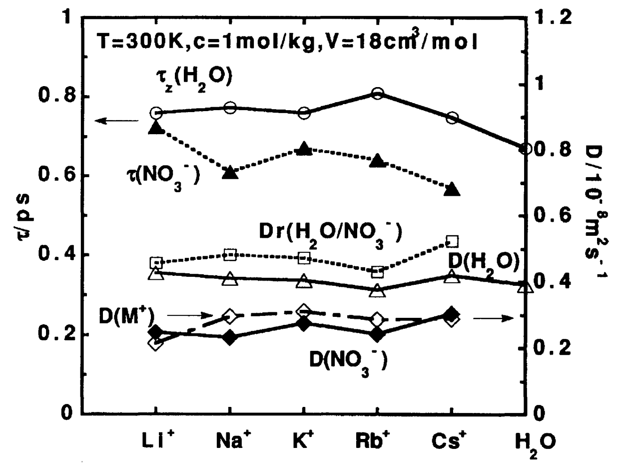

Fig. 19. Orientational relaxation time (left-hand y-axis), self-diffusion and relative self-diffusion coefficients (right-hand y-axis). $T=300$ K, $c=1$ mol kg^{-1}, $V=18$ cm^3 mol^{-1}.

are of much interest. The mean molecular distance, denoted by a, is about the same in the solution. Then a measure of the translational relaxation time is estimated as:

$$\tau(translational) = \sqrt{\frac{a^2}{6D}}. \tag{13}$$

Thus the following relation is obtained:

$$\tau(translational, \text{water}) < \tau(translational, \text{nitrate ion}). \tag{14}$$

A more detailed analysis is performed by monitoring the molecular distance between the nitrate ion and the water in its vicinity. The square of the distance is written as a linear function of time and its tangent is put as $6D^r$(water/nitrate ion) as the case of self-diffusion coefficient. The coefficient D^r is called the relative diffusion coefficient, and its value is shown in Fig. 19. Although it cannot be directly compared with the self-diffusion coefficient, it should be mentioned that the value of D^r(water/nitrate ion) is larger than D(water) numerically.

The relative diffusion coefficients of the other pairs in a $LiNO_3$ solution are described in Fig. 20 at $T=300$ K, $c=2$ mol kg^{-1}, and $V=20$ cm^3 mol^{-1}. The symbol D^r(A/B) denotes the relative diffusion coefficient for species A around species B. The quantities $D^r(Li/NO_3^-,F)$ and $D^r(Li/NO_3^-,S)$ correspond to that in the first and second neighbor, respectively. The most interesting point in this Figure is that D^r(water/water) is not small as expected from the hydrogen bonded structure. As the coefficient $D^r(Li/NO_3^-,F)$ is so small in this Figure, the departure process of Li^+ ion from the nitrate ion is slow. (It will be shown that it is not so small at $c=1$ mol kg^{-1} in Fig. 24.) From the value of $D^r(H_2O/NO_3^-)$ the increment of the H_2O–NO_3^- molecular distance is estimated to be 0.13—0.14 nm in the orientational relaxation time of the nitrate ion. This distance is long enough for water molecules to get out from the first shell of the nitrate ion (Fig. 8). This is consistent with the weak correlation between the rotation of the nitrate ion and the motion of water described in the preceding section.

The self-diffusion coefficient of water in the first shell of the nitrate ion is shown as $D(H_2O/NO_3^-)$ in Fig. 20. It is not so different from $D(H_2O)$ (average in the whole solution). This means that the translational motion of water molecules around the nitrate ion has no special feature.

Determining Factor for the Relaxation Time

In the following sections, the principal factor to determine the relaxation time of the nitrate ion is searched in reference to the microscopic quantities obtained by MD.

Correlation with *BE*(Water/Nitrate Ion). By trial error plots of the relaxation time versus a series of microscopic quantities, it turned out that the relaxation time has a strong correlation with the *BE*(water/nitrate ion) as shown in Fig. 21. In this Figure the molar volume V is 18—21 cm^3 mol^{-1} and concentration c is 1 or 2 mol kg^{-1}. The solute is $LiNO_3$–$CsNO_3$ in Table 2. The x-axis means the *BE* of water molecule around the nitrate ion.

Anisotropy of *BE*(Water/Nitrate Ion). In Fig. 22 the anisotropy of *BE*(water/nitrate ion) and D^r(water/nitrate ion) is depicted. The x-axis means the direction of the position vector of the water in the first shell that is seen from the nitrate ion (Fig. 1). The anisotropy is clearly seen in these quantities. The water in the direction C has the higher potential energy than other water molecules. For this reason this water

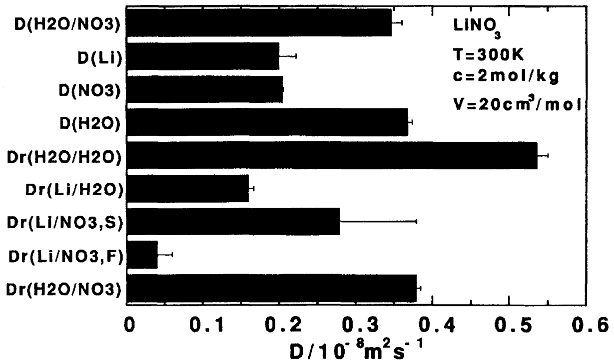

Fig. 20. Self-diffusion coefficient D and relative diffusion coefficient $D^{r}(A/B)$ for $LiNO_3$ solution. The species A is the neighbor of B. $T=300$ K, $c=2$ $mol\,kg^{-1}$, $V=18$ $cm^3\,mol^{-1}$.

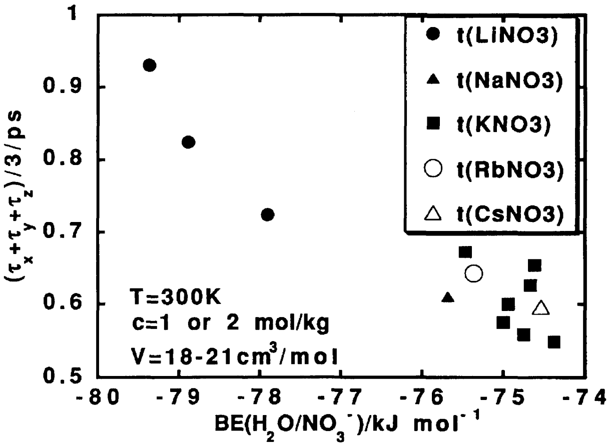

Fig. 21. Orientational relaxation time of nitrate ion versus BE(water/nitrate ion) plot.

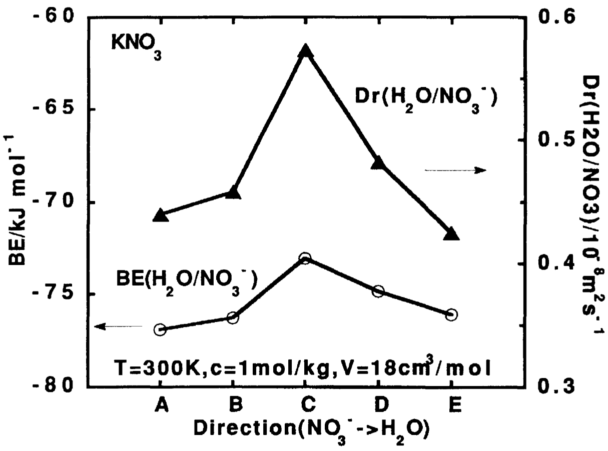

Fig. 22. Binding energy BE(water/nitrate ion) (left-hand y- axis) and relative diffusion coefficient D^{r}(water/nitrate ion) against the direction of the water seen from nitrate ion (see Fig. 1) for KNO_3 solution. $T=300$ K, $c=1$ $mol\,kg^{-1}$, $V=18$ $cm^3\,mol^{-1}$.

is easily pushed out when the nitrate ion rotates. This means that $\tau_z < \tau_{xy}$.

Several models are used to calculate the anisotropy of the relaxation time to confirm the above discussion in Table 3. The repulsion term in the pair potential is the same as the original model. The charge distribution on the "nitrate ion" is changed. The model 1 has a large anisotropy ($\tau_x/\tau_z=1.51$) and the C water has a high BE. This model is compared with model 3 where the anisotropy has the opposite trend ($\tau_x/\tau_z=0.73$) and the C water is most stable around the "nitrate ion". Our model is an intermediate one (model 2). If the charge is put to be 0, then the anisotropy is weak as shown in model 4. The effect of the anisotropy of the moment of inertia is examined by model 5 that assumes the isotropic moment of inertia. Only a 3% decrease in the relaxation time is found in both τ_x and τ_z.

Concentration Dependence. Figure 23 shows the concentration dependence of the relaxation time of the nitrate ion in $LiNO_3$ and KNO_3 solutions at $T=$ 300 K and $P=20$ MPa. The relaxation time is the average of τ_x, τ_y, and τ_z. The points at $c=0$ are the linearly extrapolated ones. Although the calculations were performed only for $c=1$ and 2 $mol\,kg^{-1}$, the linear trend is in agreement with the experiment.[3)]

The relative self-diffusion coefficients D^{r} and the inverse of the relaxation time $1/\tau$ are plotted against the concentration in Fig. 24. A clear correlation is seen between these quantities. From these results we believe that further analysis on the model solution is of much significance.

The total potential energy of the molecules surrounding the nitrate ion is the candidate to determine the relaxation time. This corresponds to a situation that the nitrate ion rotates diffusively in the water structure around the nitrate ion (see Eqs. 11 and 14).

We introduce a quantity $sumBE$ as follows:

$$sumBE = \sum_i n(i)BE(i), \tag{15}$$

where n is the coordination number. The summation is done for the first neighbor molecules and for the second neighbor cation, which is included because of the strong hydration (see $D^{r}(H_2O/Li^+)$ in Figs. 20 and 24. The τ versus $sumBE$ plot is shown in Fig. 25.

The second neighbor cation is sometimes the first neighbor of another nitrate ion. For this reason the coordination number at the second neighbor is corrected by the running coordination number $n(r_c)$ in the nitrate ion–nitrate ion pair at the distance r_c:

$$\begin{aligned} r_c &= r\left(\text{second peak of } g(r)\left(NO_3{}^{-}\text{–cation}\right)\right) \\ &\quad + r\left(\text{first peak of } g(r)\left(NO_3{}^{-}\text{–cation}\right)\right). \end{aligned} \tag{16}$$

The correction factor is $1/(1+n(r_c))$. In Table 4 both the corrected and uncorrected coordination numbers are summarized. It contains also the coordination number in the random distribution for comparison. The sum of the first and the corrected second coordination number

Table 4. Binding Energy, Coordination Number of Water and Cation around NO_3^-, and Relaxation Time at T=300 K and P=20±15 MPa

Solute		$LiNO_3$		KNO_3		Random	
V/cm^3mol^{-1}		20		21		20	
				$BE(H_2O/NO_3^-)$/kJ mol^{-1}			
c/mol kg^{-1}	1	−78.0		−75.0			
c/mol kg^{-1}	2	−79.2		−74.6			
				BE(cation)/kJ mol^{-1}			
c/mol kg^{-1}	1	−781		−512			
c/mol kg^{-1}	2	−789		−520			
				Coordination number of water n			
c/mol kg^{-1}	1	9.55		8.61		9.34	
c/mol kg^{-1}	2	9.45		8.29		9.00	
				Coordination number of cation n			
Neighbor		First	Second	First	Second	First	Second
c/mol kg^{-1}	1	0.38	0.38	0.51	0.24	0.12	0.42
			(0.76)		(0.77)		
c/mol kg^{-1}	2	0.81	0.28	0.65	0.36	0.23	0.85
			(0.77)		(1.17)		
				$sumBE$/kJ mol^{-1}			
c/mol kg^{-1}	1	−1339		−1048			
c/mol kg^{-1}	2	−1577		−1144			
				τ/ps			
c/mol kg^{-1}	1	0.74		0.59			
c/mol kg^{-1}	2	0.93		0.65			

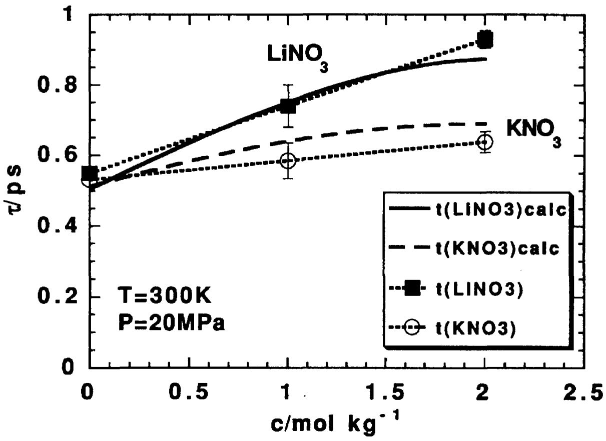

Fig. 23. Orientational relaxation time of nitrate ion $\tau=(\tau_x+\tau_y+\tau_z)/3$ versus the concentration c. The solid and dashed curves obey Eq. 18, and the dotted lines are extrapolations. T=300 K, $P\cong$20 MPa.

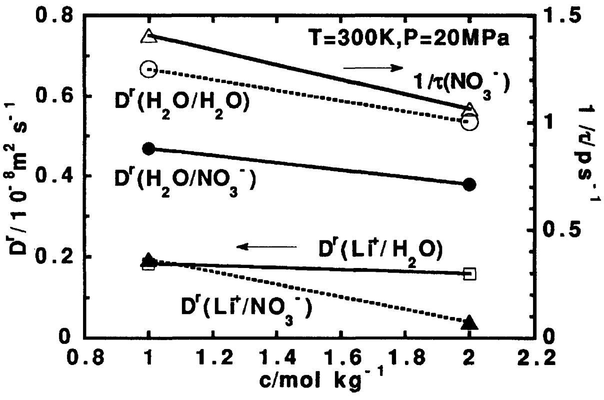

Fig. 24. Relative diffusion coefficient D^r(A/B) (left-hand y-axis) and the inverse of the relaxation time of nitrate ion $1/\tau$ (right-hand y-axis) versus the concentration c for $LiNO_3$ solution. T=300 K, $P\cong$20 MPa.

is called as the effective coordination number n of the cation. This is given in Fig. 26. The effective coordination number in the $LiNO_3$ solution is about the same with that in KNO_3 case. An empirical formula $n(c)$ can fit the MD result:

$$n(c) = c - 0.24c^2, \tag{17}$$

where the concentration c is in units of mol kg^{-1}.

In Eq. 15, BE(cation) is used which is the average over all the cations in the solution. This is adopted because the low concentration leads to poor statistics if the cation is classified. On the other hand, BE(water/nitrate ion) is accumulated in Eq. 15 because of the large number of coordination. The numerical data used in Fig. 25 are tabulated in Table 4. The points at c=0 are calculated by linear extrapolation other than the n(cation) case.

An empirical equation is used to interpolate the MD values of the relaxation time τ as a function of $sumBE$:

$$\tau = \tau_0 \exp\left(-\frac{sumBE}{E_0}\right), \tag{18}$$
$$\tau_0 = 0.31 \text{ ps}, \quad E_0 = 1515 \text{ kJ mol}^{-1}.$$

A combination of Eqs. 15, 17, and 18 gives the relax-

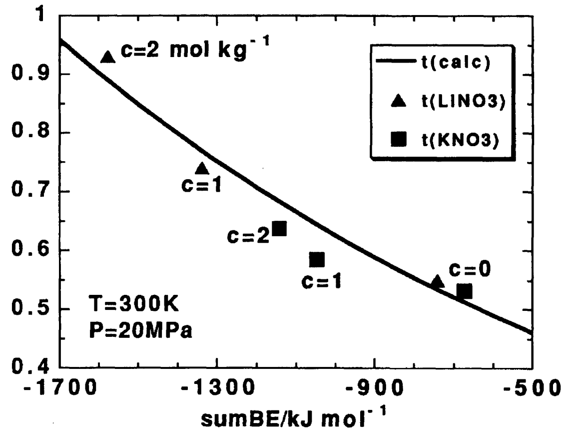

Fig. 25. Orientational relaxation time of nitrate ion $\tau=(\tau_x+\tau_y+\tau_z)/3$ versus *sumBE* (see text). The solid curve obeys Eq. 18. T=300 K, P≅20 MPa.

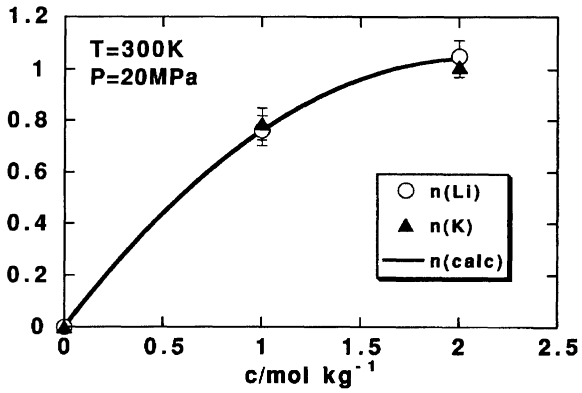

Fig. 26. Effective coordination number n of a cation around nitrate ion versus the concentration c. The solid curve obeys Eq. 17. T=300 K, P≅20 MPa.

ation time as a function of concentration c depicted by the solid and dashed curves in Fig. 23. Although these are the curves, the leading terms are linear and not far from the MD result.

The reason for the almost linear increase in the relaxation time as a function of the concentration is an energetic stabilization of the surrounding species in the present solution. The large increase in the relaxation time by addition of a small amount of salt is understood in this way. The counter cation dependence is also explained by Eq. 18.

This discussion is similar to that reported by Nicholas and Wasylishen.[2] They discussed the relative order of the cation effect (from Sc^{3+} to H_3O^+) in terms of the association of the nitrate ion with the cation. More detailed analyses are needed on both the real solution and the MD model to settle a definite picture.

Motion of Water as a Function of Concentration

In the previous section, the relaxation time of the nitrate ion was expressed as an almost linear function of c. The concentration dependence in dynamic quantities of water molecule is examined hereafter. This case is easy to calculate and compare with experiments because the low concentration limit is realized also by MD.

The results concerning the energy are plotted in Fig. 27. The potential energy E_p changes linearly with c and the *BE*(water) slightly deviates from linearity. The orientational relaxation time and the self-diffusion coefficient are shown in Fig. 28. A nonlinearity is clear in these quantities of water. In Fig. 29, the self-diffusion coefficients in a $LiNO_3$ solution are compared with those in an aqueous LiCl solution,[31] since no experiments have been reported on the diffusion in an $LiNO_3$ solution as far as the author in aware. The nonlinear dependence of D(water) is found both in the calculation and experiments. The decreasing trend with increasing c is in agreement with the experiments.

In the KNO_3 solution, *BE*(water) and D(water) increase as a function of c as shown in Fig. 30. This trend of D(water) is consistent with experiments[30] as

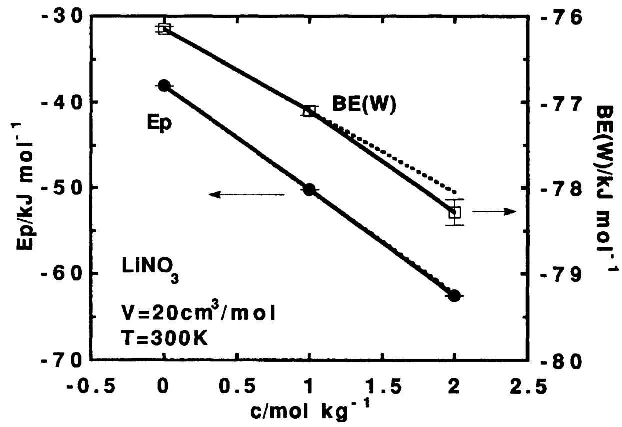

Fig. 27. Potential energy of the system E_p (left-hand y-axis) and the binding energy of water *BE*(water) against the concentration c for $LiNO_3$ solution. The dotted lines are extrapolations. T=300 K, V=20 $cm^3\,mol^{-1}$.

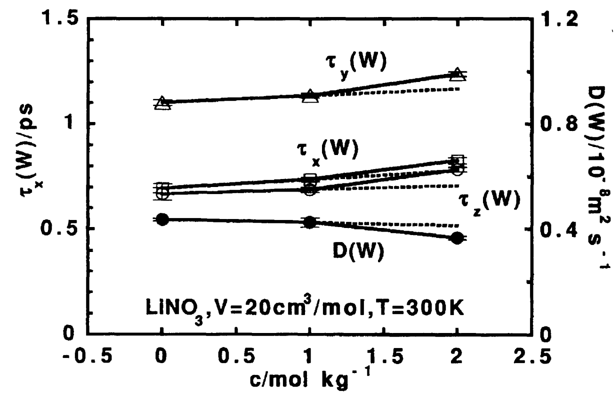

Fig. 28. Orientational relaxation time of water (left-hand y-axis) and self-diffusion coefficient (right-hand y-axis) for $LiNO_3$ solution. The dotted lines are extrapolations. T=300 K, V=20 $cm^3\,mol^{-1}$.

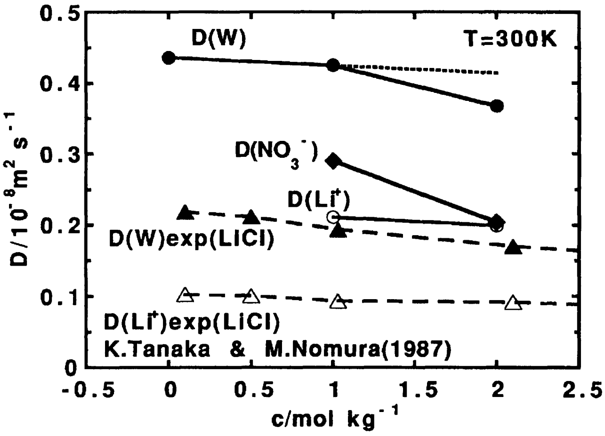

Fig. 29. Self-diffusion coefficient D versus concentration c. The calculated data for $LiNO_3$ solution ($P \cong 20$ MPa) are compared with experiments on LiCl solution.[31] The dotted line in D(W) is extrapolation. $T=300$ K.

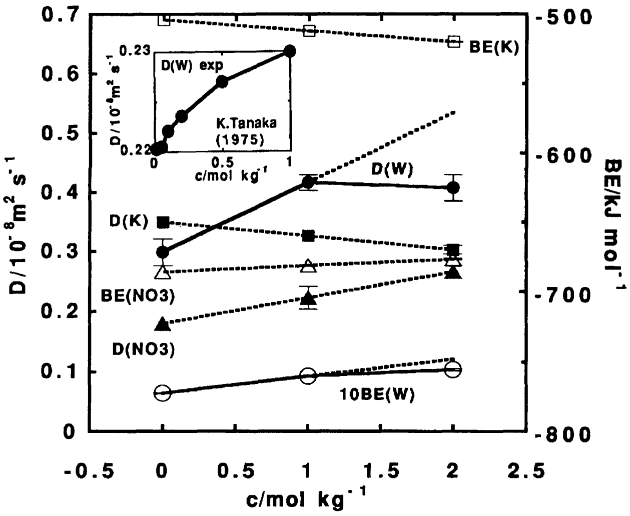

Fig. 30. Self-diffusion coefficient D (left-hand y-axis) and binding energy BE (right-hand y-axis) versus concentration c for KNO_3 solution. The dotted lines in D(W) and $10BE$(W) are extrapolations. $T=300$ K, $P \cong 20$ MPa. The inset shows the experiments.[30]

depicted in the inset.

In Figs. 28, 29, and 30, a good correspondence is found in the increasing or decreasing character of BE and D as a function of c. Thus, the behavior of D could be understood in terms of BE. Since the potential energy of water BE(water) is a result of the strong interaction mainly between water molecules, the motion of a water molecule has a strong correlation with the surrounding molecules. In this way the relaxation time and the self-diffusion coefficient exhibit a more pronounced nonlinearity than the relaxation time of the nitrate ion. Because water molecule is electrically neutral, its interaction with another water molecule is all anisotropic and it is effective both for the orientational relaxation and diffusion. In the case of the nitrate ion, having a net negative charge, the only anisotropic part is the most important in the orientational relaxation process. The total potential energy is effective in the diffusion. The relations given by Eqs. 11 and 14 are understood in this way. On the basis of this relation, it is conceivable that the nitrate ion rotates diffusively in a structure of the surrounding species that is approximated as an external field.

Pressure Dependence of Nitrate Ion Relaxation

The relaxation time of the nitrate ion in $LiNO_3$ and KNO_3 solutions is plotted in Fig. 31 against pressure at $c=2$ mol kg^{-1} and $T=300$ K. Raman experiments indicate that the relaxation time in KNO_3 solution increases as pressure increases:[9] This is also shown in Fig. 31 for comparison. The increasing trend in the calculation is too weak as compared with the experiments, and may come from the low density of the model water.[19] On the other hand the relaxation time has a shallow minimum as a function of pressure in a $LiNO_3$ solution.[33] A similar trend is seen in Fig. 31.

The coordination number versus pressure plot is given in Fig. 32. The cation and water exhibit different trends, and this is in line with the non-monotonic relaxation time as a function of pressure in Fig. 31. The decrease in the coordination number of cation in Fig. 32 is consistent with the decrease of the effective moment of inertia as revealed by Raman experiments.[9]

The author would like to thank Professor Masaru Nakahara for suggesting this problem, and Professor Nobuhiro Go for valuable discussions. He also thanks Dr. D. Fincham, Queen Mary College, and Dr. W. Smith, Science and Research Council, Daresbury Laboratory, UK for their program MDMPOL as the basis of the present program. This work has been

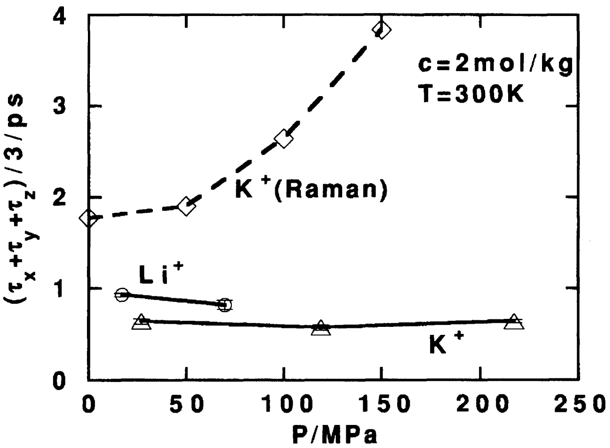

Fig. 31. Orientational relaxation time of nitrate ion $\tau=(\tau_x+\tau_y+\tau_z)/3$ versus pressure P. $T=300$ K, $c=2$ mol kg^{-1}. The rotational relaxation time observed by Raman spectroscopy[9] is also shown.

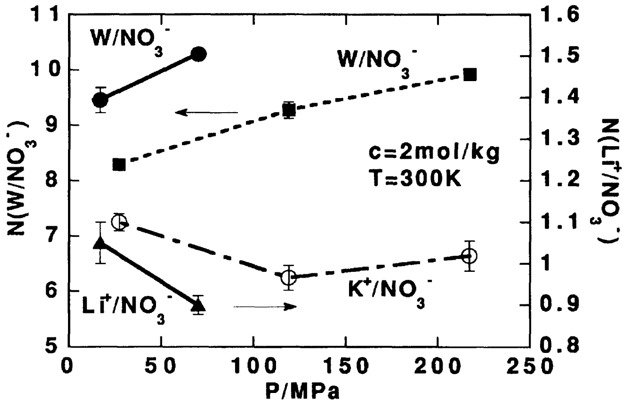

Fig. 32. Coordination number of water (left-hand y-axis) and cation (right-hand y-axis) against pressure P. T=300 K, c=2 mol kg^{-1}.

supported in part by Grants-in-Aid for Scientific Research Nos. 63430023, 01540398, 02245209, 03231211, and 04215214 from the Ministry of Education, Science and Culture. The author thanks the Computer Center of the Institute for Molecular Science for the use of HITAC M-680H and S-820/80 computers. The computation was also done with FACOM VP-400E and M-780 computers at the Kyoto University Data Processing Center.

References

1) A. M. de P. Nicholas and R. E. Wasylishen, *J. Phys. Chem.*, **89**, 5446 (1985).

2) A. M. de P. Nicholas and R. E. Wasylishen, *Can. J. Chem.*, **65**, 951 (1987).

3) A. Adachi, H. Kiyoyama, M. Nakahara, Y. Masuda, H. Yamatera, A. Shimizu, and Y. Taniguchi, *J. Chem. Phys.*, **90**, 392 (1989).

4) M. Nakahara, A. Adachi, H. Kiyoyama, A. Shimizu, Y. Taniguchi, and Y. Masuda, *J. Phys. Chem.*, **94**, 6179 (1990).

5) D. James and R. L. Frost, *Faraday Discuss. Chem. Soc.*, **64**, 48 (1977).

6) T. Kato, J. Umemura, and T. Takenaga, *Mol. Phys.*, **36**, 621 (1978).

7) M. Perrot, F. Gullaume, and W. G. Rothschild, *J. Phys. Chem.*, **87**, 5193 (1983).

8) T. Noguchi, A. Tanaka, K. Suzuki, and Y. Taniguchi, *Physica*, **139 & 140B**, 508 (1986).

9) Y. Taniguchi, T. Noguchi, and Y. Sakan, *Rev. Phys. Chem. Jpn., Special Issue Sacred to the Memory of Jiro Osugi*, 49 (1990).

10) M. Whittle and J. H. R. Clarke, *Mol. Phys.*, **44**, 1435 (1981).

11) D. R. Bauer, G. R. Alms, J. I. Brauman, and R. Pecora, *J. Chem. Phys.*, **61**, 2255 (1974).

12) R. Caminitti, G. Licheri, G. Paschina, G. Piccaluga, and G. Pinna, *J. Chem. Phys.*, **72**, 4522 (1980).

13) a) G. W. Neilson and J. E. Enderby, *J. Phys. C*, **15**, 2347 (1982); b) T. Yamaguchi, S. Tanaka, H. Wakita, and M. Misawa, *KENS Report* (National Laboratory for High Energy Physics, Oho, Tsukuba 305, Japan), **8**, 90 (1990).

14) K. Ibuki and M. Nakahara, *J. Chem. Phys.*, **90**, 386 (1989).

15) N. Lee, R. G. Keesee, and A. W. Casleman, Jr., *J. Chem. Phys.*, **72**, 1089 (1980).

16) M. P. Tosi and F. G. Fumi, *J. Phys. Chem. Solids*, **25**, 45 (1964).

17) a) T. Yamaguchi, I. Okada, H. Ohtaki, M. Mikami, and K. Kawamura, *Mol. Phys.*, **58**, 349 (1986); b) J. F. Wyatt, I. H. Hillier, V. R. Saunders, and J. A. Conner, *J. Chem. Phys.*, **54**, 5311 (1971).

18) V. Carravetta and E. Clementi, *J. Chem. Phys.*, **81**, 2646 (1984).

19) Y. Kataoka, *J. Chem. Phys.*, **87**, 589 (1987).

20) Y. Kataoka, *Bull. Chem. Soc. Jpn.*, **62**, 1421 (1989).

21) W. Smith and D. Fincham, "CCP5 Newsletter," an informal letter freely available from Science & Research Council, Daresbury Laboratory, Warrington WA4 4AD, England.

22) K. Krynicki, *Physica*, **32**, 167 (1966).

23) D. W. G. Smith and J. G. Powles, *Mol. Phys.*, **10**, 451 (1966).

24) J. A. Glasel, *Proc. Natl. Acad. Sci. U. S. A.*, **55**, 479 (1966).

25) K. Heinzinger and P. C. Vogel, *Z. Naturforsch., A*, **31a**, 463 (1976).

26) P. C. Vogel and K. Heinzinger, *Z. Naturforsch., A*, **31a**, 476 (1976).

27) P. Bopp, W. Dietz, and K. Heinzinger, *Z. Naturforsch., A*, **34a**, 1424 (1979).

28) H. Yokayama, private communication.

29) H. Yokayama and T. Ohta, *Bull. Chem. Soc. Jpn.*, **61**, 3073 (1988).

30) K. Tanaka, *J. Chem. Soc., Faraday Trans. 1*, **71**, 1127 (1975).

31) K. Tanaka and M. Nomura, *J. Chem. Soc., Faraday Trans. 1*, **83**, 1779 (1987).

32) R. Mills, *J. Am. Chem. Soc.*, **77**, 6116 (1955).

33) Y. Sakan, A. Shimizu, and Y. Taniguchi, unpublished results.